

Transition Probabilities for the Prominent Red Lines of Ne I

J. M. Bridges and W. L. Wiese

National Bureau of Standards, Washington, D. C. 20234

(Received 16 March 1970)

Relative transition probabilities of all 30 lines belonging to the prominent $3s$ - $3p$ transition array of Ne I have been measured in emission with a wall-stabilized arc operating in an argon-neon mixture at atmospheric pressure. The data have been normalized to an absolute scale provided by recent lifetime measurements of the $3p$ levels. Our results, as well as the data from other emission measurements, have been subjected to extensive comparisons and tests, including a check for fulfillment of the J -file sum rule. It is found that our data exhibit a much better consistency than any other set of individual values. On the basis of this analysis as well as our uncertainty estimates, we estimate that the accuracy of our individual transition probabilities for this transition array, except for a few weak lines, is of the order of 10% on an absolute basis.

INTRODUCTION

The transition probabilities of the prominent red lines of Ne I, which comprise the $3s$ - $3p$ transition array, have been the object of numerous studies. A critical compilation of available data¹ undertaken by one of us several years ago made use of eight experiments²⁻⁹ and one theory.¹⁰ Nevertheless, the "best values" obtained from this study were estimated to have accuracies of no more than 10-25%. More recently, 11 new transition-probability measurements¹¹⁻²¹ for these transitions were reported, in which a variety of experimental techniques was applied, including measurements of lifetimes,¹¹⁻¹⁸ emission intensities,¹⁸⁻²⁰ and an application of the Faraday effect.²¹

Among these investigations, the numerous lifetime experiments serve principally to establish the absolute scale, since they provide transition probability sums from the measured upper levels, but - except for the special case of the 6402-Å line - no individual values. The absolute scale was first reliably established several years ago from the lifetime work of Klose,⁸ with an accuracy of about 10%. The more recent lifetime experiment of Bennett and Kindlmann¹⁷ has narrowed the uncertainties down to 3-5%. The principal advance in this new experiment is the elimination of cascading effects by using threshold energy excitation.

While the absolute transition probability sums are thus very accurately determined, the individual (relative) values obtained from the other above-mentioned experimental techniques have not yet been nearly as precise. This is somewhat an anomalous situation as regards atomic f values, since normally the (relative) individual f values of lines within a transition array (especially of course when LS-coupling prevails) are very accurately

established, while the absolute scale is much more in doubt. The most recent measurements of relative individual values exhibit still some large disagreements with each other - up to 55%, violate the J -file sum rule, and are inconsistent with the lifetime results, as far as the ratios of the transition-probability sums from different upper levels are concerned.

It appears, therefore, that a precise determination of the relative individual line data is very desirable in order to match and make full use of the accurately measured absolute transition-probability sums. This has been the principal motivation for undertaking this work. Measurements in emission are called for because these, as well as the lifetime measurements, start with an upper level as the initial state. The measurements of the relative transition probabilities for all transitions from a given upper level represent, furthermore, an especially simple and precise application of the emission method, since such intensity measurements, confined to the same upper level, are practically independent of the conditions of the emitting source. Only the condition that the source is optically thin needs to be checked. No assumptions about the existence of local thermal equilibrium (LTE) are necessary, and no temperature or particle-density measurements are required. But also, for linking up all the emission measurements from the various $3p$ levels, which have an energy spread of 5%, the conditions in the plasma source do not enter sensitively into the measured data. This follows mainly from the circumstance that the small spread in the excitation energies makes all lines almost equally temperature dependent. Therefore, accurate relative f values are to be expected from such emission measurements if modern precise data-acquisition techniques are applied.

EXPERIMENTAL METHOD

We have followed the standard method of line emission measurement²²: The transition probabilities A_{ki} of lines of a given species are related to the emitted line intensities by

$$A_{ki} = [U(T)/Ng_k]I_{ki}e^{E_k/kT}(1/l), \quad (1)$$

assuming an optically thin layer and the presence of LTE. The $U(T)$ is the partition function of the species, E_k is the energy, g_k is the statistical weight of the upper level k , N is the number density of the species, I_{ki} is the emitted intensity for a transition to lower level i (in photons \times sec⁻¹ cm⁻²), and l is the length of the emitting layer. Since we want to determine in this experiment only relative A values for lines of a given species, we need only measure relative intensities, and determine the value of T .

The source for our measurements was a wall-stabilized arc operating with a neon-argon mixture at atmospheric pressure. The arc was run at currents of 40 and 70 A. The water-cooled copper discs for constricting the arc column were 6.5 mm thick and separated from each other by 2.5-mm-thick insulator rings; the constricting holes were of 5-mm diameter. The neon and argon gases, obtained from separate cylinders, were mixed together in a small chamber during a run, and the mixture admitted to the arc chamber at slightly above atmospheric pressures at a rate of approximately 200 ml/min. The arc was imaged side-on with a concave mirror onto the entrance slit of a 2.25-m Ebert spectrometer with a 1800-line/mm grating blazed at 5000 Å. Light coming through the exit slit of the spectrometer was detected with a phototube having S-20 response. (For the 8082-Å line, a cooled tube with S-1 response was substituted.) A filter was used to block out second-order radiation coming through the spectrometer. The amplified signal was displayed on a strip-chart recorder and for some runs also recorded on paper tape for input to an electronic computer. The neon lines were first observed by scanning over the spectrum using slit widths of 30 μm. The lines all appeared to be quite narrow (with half-widths less than 0.2 Å), superposed on top of a continuum. On increasing the ratio of neon to argon, the continuum practically disappeared, indicating that it was almost entirely due to argon. Also, as the neon to argon ratio was increased (while keeping the arc current constant) the intensity of the neon lines first increased approximately in proportion to the neon concentration; however, as a pure neon arc column was approached, the neon line intensities increased at a much greater rate. After these observations, further runs were made

with large admixtures of argon; the exact amount varied somewhat for different runs, but this was of no consequence since each run was independently calibrated. Under these conditions the neon and argon densities as well as the temperature remained very steady during a run. This was demonstrated by the fact that line intensity measurements repeated during a run agreed with each other to within $\pm 2\%$ or better.

Since the neon lines are relatively narrow, it is important to check whether self-absorption is occurring to any significant extent, i.e., a few percent or more. This effect could, if present, be eliminated by decreasing the neon-to-argon ratio. (The Ar-Ne mixture rather than a pure Ne plasma was used, mainly to avoid self-absorption). To check for self-absorption, a concave mirror was placed behind the arc in the extension of the optical path. This mirror focused the arc back into itself, effectively doubling the length of the emitting volume. For optically thin lines, i.e., no self-absorption, the intensity received will be doubled, whereas a smaller increase in signal indicates that self-absorption is occurring. Light losses by reflection were, of course, taken into account. For the conditions under which we were operating, all the measured lines were found to be optically thin by the test just described. As an additional check, some lines were measured at arc currents of both 40 and 70 A. Self-absorption should result in the intensity ratio of a strong to a weak line being somewhat decreased at the higher current, where the self-absorption in the strong line would be more pronounced. But all measured ratios were the same for lines from the same energy levels, indicating again that the lines were optically thin.

For the first runs, we were only concerned in obtaining relative intensities among lines emitted from the same atomic level. Thus for these measurements, spatial resolution of the arc was unnecessary; we merely integrated all the light from across an arc diameter. For the first few runs, the line intensities were obtained from the strip-chart records by measuring the area under each line profile with a planimeter. For subsequent runs, the slits were opened to ≥ 300 μm so as to include essentially all the line intensity within the wavelength bandpass of the instrument. Scanning over the lines then gave a rectangular profile – the height of the rectangle being a measure of the line intensity. With a large ratio of slit width to linewidth, the wing correction (i.e., correction for line intensity in the far wings not passed by the spectrometer) was quite small, on the order of 10%. Furthermore, the linewidths for all 3s-3p lines are approximately the same. Since we measure intensity ratios, the wing corrections thus es-

sentially cancel out in the data analysis.

To determine the wavelength response of the spectrometer-detector system, we used a calibrated tungsten strip lamp. After each arc run, the lamp was placed at the arc position and the lamp intensity was measured at the wavelength of each line.

For connecting lines from different upper levels to a common relative scale, the temperature T needs to be determined. This in turn requires spatial resolution of the arc in order to be able to obtain the emission from a small volume element where the temperature has a unique value. We have applied the standard technique of driving the arc image across the spectrometer entrance slit so that a (projected) spatial arc profile is obtained. The Abel inversion is then performed on these data using a digital data-processing system²³ to give the radial intensity profile.

The temperature is then determined as follows: The standard arc conservation and equilibrium laws,²⁴ which include the Saha equations, Dalton's law, and the quasineutrality condition, furnish several relations between the unknown temperature and particle densities. It turns out that for the Ar-Ne mixture, as for any two-component mixture, the number of unknowns exceeds the number of equations by 2. (We assume, of course, that the mixing ratio of Ne to Ar is unknown, since it is well known that the density ratio within the arc column may change from that which was admitted into the arc chamber.) The two missing relationships may be provided from line intensity measurements. If Eq. (1) is applied to an Ar and a Ne line of known transition probability and their intensities are measured on an absolute basis, then one obtains two additional numerical relations between the unknown temperature and particle densities, so that one may solve simultaneously for all unknown quantities.

The two lines employed for the intensity measurements are the Ar Γ line at 6965 Å and the Ne Γ line at 5852 Å. For the latter we have used an A value of $6.86 \times 10^7 \text{ sec}^{-1}$, which was obtained from Bennett's lifetime value for the $2p_1$ level combined with the relative values that we measured for the two lines originating from this level.

The value of electron density was found to be about 10^{16} cm^{-3} . This makes our assumption of LTE, based upon available equilibrium criteria,²⁴ only marginally justified. Experiments,^{25,26} on the other hand, indicate that in Ar arcs the LTE still exists at an electron density of 10^{16} cm^{-3} and that deviations become noticeable only below this number.

As was discussed earlier, however, the closeness of the upper energy levels of the lines that

we are comparing results only in a rather insensitive dependence of the relative A values on temperature. The errors in the transition probabilities introduced by marginal LTE validity and uncertainties in the temperature determination are therefore quite small, typically 1–3%. This is also borne out by our results, which show no systematic trend with energy level when compared with the accurate lifetime measurements of Bennett.

RESULTS AND DISCUSSIONS

The following comparisons and tests are primarily concerned with relative transition probabilities and their distribution within the transition array, since our measurements have yielded relative values only. However, as a matter of convenience and to make our data more useful, they are usually given in the absolute scale adopted below. In Table I we present the measured transition probabilities, with the transitions being arranged in such an order that those starting from the same upper energy level are grouped together, and the upper levels are listed in order of the convenient Paschen notation. (In this notation the $3s$ levels are denoted by $1s_m$ and the $3p$ levels by $2p_n$.) We have used this particular arrangement since the intensity ratios for lines starting from the same upper energy level are independent of the conditions of the light source (assuming that there is no self-absorption). Systematic errors for the transition probabilities in each of the line groups are therefore minimal. For the normalization of our data to an absolute scale, two possibilities avail themselves. (i) The measured arc temperature may be used in combination with the Boltzmann factors for the (relative) level populations [see Eq. (1)] to put the lines on a common relative scale. The data may be then converted to an absolute scale by normalizing our total transition-probability sum for all $3s$ - $3p$ lines to the total transition-probability sum obtained from the lifetime measurements for all $3p$ levels of Bennett and Kindlmann.¹⁷ This approach assumes that LTE exists, but the results are rather insensitive to this assumption since the upper levels of the transitions lie within a narrow energy range. The resulting transition probabilities are listed in column 5 of Table I as "This expt. I." (ii) We may also normalize our transition probability sums from each p level independently with Bennett's respective individual lifetimes. The data obtained from this approach are listed in the last column of Table I as "This expt. II." They are found to be somewhat less consistent with the J -file sum rule (to be discussed later) than the data set I. Therefore only set I will be applied to all further comparisons and it is our recommended set of data.

TABLE I. Results and comparison with other recent emission experiments and the critical-data compilation NSRDS-NBS 4. To allow a convenient comparison of the *relative* transition probabilities, all data sets are forced to agree for the s_2-p_1 transition. The recommended set of data from this experiment is given in column 5 as "This expt. I."

Transition	λ	g_i	g_k	Transition probabilities [10^7 sec^{-1}]						
				This expt. ^a I	Bengtson and Miller (Ref. 20) ^b	Doherty (Ref. 5) ^c	Nodwell <i>et al.</i> (Ref. 18) ^d	Fried- riches (Ref. 7) ^e	NSRDS- NBS 4 (Ref. 1) ^f	This expt. ^a II
s_4-p_1	5400.56	3	1	0.090	0.13	0.088
s_2	5852.49	3	1	7.06	7.06	7.06	7.06	7.06	7.06	6.86
s_5-p_2	5881.90	5	3	1.02	1.18	1.39	1.06	1.13	1.26	1.04
s_4	6030.00	3	3	0.512	0.60	0.61	...	0.55	0.616	0.523
s_3	6163.59	1	3	1.41	1.68	1.57	1.45	1.77	1.57	1.44
s_2	6598.95	3	3	2.25	2.36	2.40	2.40	...	2.46	2.30
s_4-p_3	6074.34	3	1	5.83	5.71	6.1	6.22	6.94	6.06	5.65
s_2	6652.09	3	1	0.034	0.033
s_5-p_4	5944.83	5	5	1.12	1.04	1.19	1.06	1.09	1.03	1.13
s_4	6096.16	3	5	1.79	1.67	1.80	1.80	...	1.66	1.80
s_2	6678.28	3	5	2.31	2.56	2.12	2.25	...	2.34	2.31
s_5-p_5	5975.53	5	3	0.349	0.38	0.48	...	0.54	0.425	0.341
s_4	6128.45	3	3	0.070	0.321	0.068
s_3	6266.50	1	3	2.54	2.28	2.42	2.18	...	2.19	2.49
s_2	6717.04	3	3	2.17	2.48	2.14	2.15	...	2.30	2.12
s_5-p_6	6143.06	5	5	2.85	2.67	2.70	2.36	...	2.12	2.88
s_4	6304.79	3	5	0.424	0.47	0.54	0.52	0.47	0.498	0.427
s_2	6929.47	3	5	1.74	2.04	1.62	1.77	...	1.87	1.76
s_5-p_7	6217.28	5	3	0.601	0.92	0.71	0.75	0.91	0.763	0.602
s_4	6382.99	3	3	3.16	2.22	3.05	3.19	...	2.74	3.16
s_3	6532.88	1	3	1.06	1.49	1.41	1.08	...	1.26	1.06
s_2	7024.05	3	3	0.196	0.195
s_5-p_8	6334.43	5	5	1.80	1.41	1.69	1.58	...	1.34	1.78
s_4	6506.53	3	5	2.98	2.46	2.62	2.64	...	2.28	2.95
s_2	7173.94	3	5	0.321	0.44	0.28	0.359	0.317
s_5-p_9	6402.25	5	7	5.06	...	5.4	4.25	5.15
s_5-p_{10}	7032.41	5	3	2.53	1.99	2.14	2.13	...	1.89	2.70
s_4	7245.17	3	3	1.00	0.92	0.85	1.03	...	0.960	1.07
s_3	7438.90	1	3	0.242	0.37	0.28	0.287	0.258
s_2	8082.46	3	3	0.012	0.013

^aEstimated uncertainty in relative values $\pm 7\%$, except for 5400-, 6652-, 6128-, and 8082-Å lines, where it is 15%.

^bEstimated uncertainty in relative values $\pm 10\%$, and 50% for 7439-Å line.

^cEstimated uncertainty in relative values $\pm 10\%$, except 20% for 7174-Å and factor of 2 for 7439-Å lines.

^dEstimated over-all uncertainty between 5 and 13%.

^eEstimated uncertainty for relative values between 19 and 27%.

^fEstimated uncertainty for relative values between 10 and 20%.

Our estimated errors include the measurement errors, uncertainties in the temperature determination, and uncertainties in the wavelength-dependent factors in the calibration.

We also present in Table I selected comparison data. We could have compared our results with all the experimental work listed in the introduction, but have confined ourselves to the presentation of other recent emission experiments, since this very similar work may be most directly compared with our results. In addition to the emission experiments we list also the critically evaluated

data of Ref. 1, in which by a "best-fit" technique the best earlier experimental results are combined. Since our prime concern is a convenient comparison of the individual (relative) f values, we have arbitrarily renormalized all data sets to be in exact agreement for the 5852-Å transition. One should expect close agreement between the four emission measurements of Friedrichs,⁷ Nodwell *et al.*,¹⁸ Doherty,⁵ and Bengtson and Miller,²⁰ since they are all based on essentially the same experimental method. Especially for the line groups starting from a given upper level, the

agreement should be excellent since significant systematic errors are minimized. The results show nevertheless some large disagreements of up to 55% (see the s_2-p_8 and s_4-p_7 transitions) which are far outside the estimated error limits. This was quite surprising and has been the principal reason for undertaking this work. On first examination it appears that our results do not improve the situation. Fortunately, the various sets of data may be subjected to several tests and spectroscopic checks which we feel clearly indicate that our measurements are the most accurate ones. This analysis, which will be now discussed in detail, should be more reliable than the various error estimates which, as the comparisons have shown, are not too realistic.

We first have to collect some basic relationships and expressions for the atomic transition probability A and the line strength S . The two quantities are related by

$$A_{ki} = \frac{64\pi^4}{3h^3\lambda^3} \frac{S}{2J_k+1}, \quad (S \text{ in atomic units}) \quad (2)$$

and S may be in the standard central field approximation expressed by an angular factor $\mathfrak{S}(L)$ and a radial factor, usually denoted by σ^2 , so that

$$S = \mathfrak{S}(L)\sigma^2. \quad (3)$$

The subscripts i and k indicate the lower and upper level, respectively; λ is the wavelength; and J is the total angular momentum quantum number. $\mathfrak{S}(L)$ represents the relative strength of a transition. When LS coupling prevails, $\mathfrak{S}(L)$ may be expressed as $\mathfrak{S}(\mathfrak{M})\mathfrak{S}(\mathfrak{L})$, where $\mathfrak{S}(\mathfrak{M})$ is a relative multiplet strength, and $\mathfrak{S}(\mathfrak{L})$ is a relative line strength. The two quantities are for LS coupling readily determined theoretically and are available from general tabulations.^{27,28} The investigated transition array of Ne I is, however, far from this simple coupling case (or from any other pure coupling), so that it becomes very difficult to calculate accurate individual line strengths. Only Mehlhorn's recent calculations²⁹ agree well with the experimental data.^{29,30} This, of course, has been one of the underlying reasons for all the experimental work on these lines.

The radial transition integral σ^2 is given by

$$\sigma^2 = [1/(4l_g^2 - 1)] \left[\int r R(n, l) R(n', l') dr \right]^2. \quad (4)$$

The r is the radial distance; l is the orbital angular momentum quantum number and n is the principal quantum number for the initial state; n' and l' are the same quantities for the final state. $R(n, l)/r$ and $R(n', l')/r$ (normalized in atomic units) are the radial wave functions of the optical electron in its initial and final state. l_g is the greater of the two orbital angular momentum quantum num-

bers involved.

One observes that σ^2 depends (in the central-field approximation) only on n , l , n' , and l' . It follows that it is invariant for a given transition array, such as $3s-3p$ of Ne I considered here.

We may use this result in conjunction with the J -file sum rule as a first check of the data. The J -file sum rule, first derived by Shortley,³¹ states that the line-strength sums of the various J files within a transition array are in the ratios of the respective statistical weights $2J+1$. Thus we have the proportionalities

$$\sum_i S(i, k) \propto 2J_k + 1 \quad \text{and} \quad \sum_k S(i, k) \propto 2J_i + 1. \quad (5)$$

Specifically for an $s-p$ array, one may derive from Shortley's paper

$$\begin{aligned} \sum_s S(s, p) &= (2J_p + 1)\sigma^2, \\ \sum_p S(s, p) &= 3(2J_s + 1)\sigma^2, \end{aligned} \quad (6)$$

where σ^2 is constant for the array, as was seen above.

This rule may be readily applied to the data listed in Table I, since these cover – with the exception of Friedrich's data⁷ – essentially the complete transition array. For this purpose we have first rearranged our data [expressed now in line strengths $S(s_m, p_n)$] in the array presented in Table II. Each row, i.e., each p level, and each column, i.e., each s level, has its individual J and represents a J file. The measured line-strength sums $\sum_m S(s_m, p_n)$, given on the right-hand side of the Table, and $\sum_n S(s_m, p_n)$, given at the bottom, should be according to Eqs. (5) in the ratios of the statistical weights $2J+1$, which are tabulated immediately next to them. It is observed that this rule is indeed very well fulfilled by our data.

We have then, as the second step, subjected the slightly incomplete data of Bengtson and Miller,²⁰ Nodwell *et al.*,¹⁸ and Doherty⁵ to the same test. The resulting line-strength sums for the ten $3p$ levels and the four $3s$ levels are given in Table III and may be compared with the J -file sum-rule expectations as well as our own results. To allow convenient comparisons, we have reduced the line-strength data in this table in such a way that the over-all line-strength sum $\sum_m \sum_n S(s_m, p_n)$ is made equal to the over-all sum of the statistical weights $\sum 2J_{p_n} + 1$. If all lines are measured, the total sum of the statistical weights amounts to 36; the normalization is also possible on a partial basis by summing over those levels for which all lines have been measured. The same normalization may be performed via the s levels; here, however, the statistical weights must be multiplied by a factor of 3 [see Eq. (5)] to be consistent. It is evident that our results fulfill the J -file sum rule far bet-

TABLE II. Measured line strengths S (normalized as in Table I), J -file sums $\sum S(s_m, p_n)$, and statistical weights $2J_{p_n} + 1$.

Upper level	Lower level	Line strengths (atomic units)				J -file sums $\sum_m S(s_m, p_n)$	Statistical weights $2J_{p_n} + 1$
		s_2	s_3	s_4	s_5		
$2p_1$	6.98	...	0.0700	...	7.05	1	
$2p_2$	9.57	4.87	1.66	3.07	19.17	3	
$2p_3$	0.0496	...	6.43	...	6.48	1	
$2p_4$	16.9	...	10.0	5.83	32.73	5	
$2p_5$	9.74	9.26	0.237	1.10	20.34	3	
$2p_6$	14.3	...	2.61	16.3	33.21	5	
$2p_7$	1.00	4.38	12.2	2.13	19.71	3	
$2p_8$	2.93	...	20.3	11.3	34.53	5	
$2p_9$	45.9	45.9	7	
$2p_{10}$	0.0940	1.47	5.63	13.0	20.19	3	
$\sum_n S(s_m, p_n)$	61.56	19.98	59.14	98.63	$\sum_m \sum_n S = 239.31$		
$2J_{s_m} + 1$	3	1	3	5			

ter than those of any of the other authors, including the critical NBS compilation.¹ The average deviation from the individual J -file sums for our data set I is only 2.0%, while the corresponding numbers for the others are: Nodwell *et al.*, 6%; Bengtson and Miller, 9%; Doherty, 5%; NSRDS-NBS 4, 8%; and our data set II, 2.6%.

As mentioned above, the J -file sum rule holds only approximately insofar as it is based on the assumption of a common value for σ^2 within a transition array. Appreciable variations of σ^2 within a transition array may occur if configuration-interaction effects become significant or if the transition integral is sensitive to the slightly

varying wave functions of the individual levels within the array. Neither seems to be the case for the $3s-3p$ array of Ne I: First, from an examination of the energy-level structure for Ne I one would not expect any significant configuration interaction since the levels most likely to interact are a good distance apart. Second, all lifetime measurements indicate a large value of σ^2 for this array. Normally only small values of σ^2 are significantly affected by slight variations in the wave functions.

The Coulomb approximation,¹⁰ as a central-field approximation, yields basically one value for σ^2 per transition array. But it is also a semiempirical method, with experimental energy levels as input, which allows therefore the calculation of individual σ^2 values for each of the transitions of the array. Variations in σ^2 may thus indicate the presence of a significant amount of configuration interaction. We find, however, only a very small variation in the σ^2 data, with an average deviation of 1.5%. In Table IV we list for each p level an average value of σ^2 from the Coulomb approximation by weighting it according to the strengths of the contributing transitions. We present then for comparison the σ^2 values obtained from our measurements as well as those from the emission experiments of Bengtson and Miller,²⁰ Nodwell *et al.*,¹⁸ and Doherty.⁵ The experimental values are obtained with the help of Eq. (6). For convenient comparison, all σ^2 values for the $2p_1$ level are normalized to a value of 7.1 (which corresponds to our

TABLE III. Relative J -file sums $\sum_m S(s_m, p_n)$ and $\sum_n S(s_m, p_n)$. The data are reduced in such a way that the over-all line-strength sum $\sum_m \sum_n S(s_m, p_n)$ is made equal to the over-all sum of the statistical weights $\sum_n 2J_{p_n} + 1$.

$2p_n$ levels	$2J_{p_n} + 1$	This expt. I	Nodwell (Ref. 18)	Bengtson and Miller (Ref. 20)	Doherty (Ref. 5)	NSRDS-NBS 4 (Ref. 1)
$\sum_m S(s_m, p_n) \sim (2J_{p_n} + 1)$						
$2p_1$	1	1.06	1.14	1.09	1.06	1.15
$2p_2$	3	2.88	3.02	3.30	3.31	3.57
$2p_3$	1	0.976	1.13	0.98	1.02	1.10
$2p_4$	5	4.92	5.26	5.16	4.82	5.21
$2p_5$	3	3.06	2.88	...	3.03	3.39
$2p_6$	5	4.99	5.11	5.41	4.87	5.01
$2p_7$	3	2.96	3.17	2.77	3.04	3.02
$2p_8$	5	5.20	4.55	4.56	4.71	4.46
$2p_9$	7	6.91	7.49	6.33
$2p_{10}$	3	3.04	2.74	2.73	2.65	2.76
Sums	36	36.00	29.00 ^a	26.00 ^a	36.00	36.00
$\sum_n S(s_m, p_n) \sim 3 \times (2J_{s_n} + 1)$						
s levels	$2J_{s_m} + 1$					
$1s_2$	9	9.26	9.47	10.42	8.83	10.42
$1s_3$	3	3.01	2.85	3.47	3.31	3.34
$1s_4$	9	8.89	9.19	...	8.55	8.79
$1s_5$	15	14.84	15.31	13.45
Sums	36	36.00	36.00	36.00

^aPartial sums for the transitions covered by the measurements.

TABLE IV. Average values of the radial transition integrals σ^2 for transitions starting at the indicated levels. For convenience of comparison, the data of Bengtson, Doherty, and Nodwell *et al.* are normalized to our value for the $2p_1$ level.

Upper-level Paschen notation	Coulomb approximation [10]	Bengtson and Nodwell			
		This expt. I	Miller (Ref. 20)	Doherty (Ref. 5)	<i>et al.</i> (Ref. 18)
$2p_1$	6.2	7.1	7.1	7.1	7.1
$2p_2$	6.5	6.4	7.1	7.4	6.3
$2p_3$	6.3	6.5	6.3	6.8	7.0
$2p_4$	6.5	6.5	6.7	6.5	6.6
$2p_5$	6.5	6.8	...	6.8	6.0
$2p_6$	6.5	6.6	7.0	6.5	6.4
$2p_7$	6.4	6.6	6.0	6.8	6.5
$2p_8$	6.5	6.9	5.9	6.3	5.6
$2p_9$	6.4	6.6	...	7.2	...
$2p_{10}$	6.5	6.7	5.9	5.9	5.6

line-strength value of Table II). It is seen that our measurements give excellent agreement with the Coulomb approximation throughout the array. On the other hand, a trend toward smaller values with increasing n of the $2p_n$ levels is noticed in the data of Bengtson and Miller and Nodwell *et al.* Some possible explanations for the occurrence of such trends will be discussed later.

As another major test one may check how our relative transition probability sums for the various p levels compare with the accurate lifetimes measured by Bennett and Kindlmann.¹⁷ The lifetimes for the p levels are related to the transition probabilities by

$$\tau_{p_n} = 1 / \sum_m A(s_m, p_n), \quad (7)$$

where the summation extends over all s levels for which transitions to the p levels are allowed.

In Table V, our measured transition-probability sums, i.e., the inverse lifetimes, as well as those from the other recent emission measurements, are compared with the data obtained directly by Bennett and Kindlmann,¹⁷ Klose,⁸ Denis,¹¹ Bakos,¹² and Osherovich *et al.*¹⁴ from their lifetime measurements. We are again primarily concerned with the relative distribution of the data over the various p levels, not with the absolute scale. The following was observed. (i) Our values maintain excellent agreement with Bennett and Kindlmann¹⁷ throughout all ten p levels. This is quite significant since Bennett's transition-probability sums for the p levels are all independently measured, while our transition-probability sums are interconnected through a common temperature value. (ii) A very closely agreeing set of inverse lifetimes is obtained if the radial transition integrals from the Coulomb approximation,¹⁰ averaged for each group of transitions starting from a given p level, are used to normalize our respective relative values. In this case our data are used only for each group of lines starting from a given p level, while the connection between different p levels is done by the Coulomb approximation. (iii) Against the excellent agreement of these three sets of data, all other available numbers show appreciably greater scatter and, partly, also a systematically different behavior.

In Fig. 1 we have illustrated this situation graphically. In addition to the numbers from the Coulomb approximation,¹⁰ from Bennett and Kindlmann,¹⁷ and from our work, we have selected the numbers of Klose⁸ and Doherty⁵ as they are the best of the other lifetime and emission measurements. (This selection is necessary in order not to overload the graph.) It is seen that Klose's and Doherty's data show significantly larger irregular-

TABLE V. Comparison of transition-probability sums [10^7 sec^{-1}].

Upper level	Lifetime experiments					Emission experiments				Theory
	This expt.	Bennett <i>et al.</i> (Ref. 17)	Klose (Ref. 8)	Denis <i>et al.</i> (Ref. 11)	Bakos and Szigeti (Ref. 12)	Osherovich and Verolainen (Ref. 14)	Bengtson and Miller (Ref. 20)	Nodwell <i>et al.</i> (Ref. 18)	Doherty (Ref. 5)	Coulomb approximation (Ref. 10)
$2p_1$	7.15	6.95	6.80	6.92	6.76	7.1	7.06 ^a	7.06 ^a	7.06 ^a	6.65
$2p_2$	5.19	5.32	5.95	5.07	2.2	5.0	5.82	...	5.97	5.59
$2p_3$	5.86	5.69	4.29	3.94	3.55	5.5	5.71 ^a	6.22 ^a	6.1 ^a	6.04
$2p_4$	5.22	5.23	4.47	3.81	3.56	4.2	5.27	5.11	5.11	5.48
$2p_5$	5.13	5.02	5.30	5.35	3.82	4.4	5.14 ^a	...	5.04 ^a	5.21
$2p_6$	5.01	5.07	4.55	3.46	4.55	4.8	5.18	4.65	4.86	5.20
$2p_7$	5.02	5.03	4.93	4.95	...	4.5	5.19
$2p_8$	5.10	5.04	4.12	3.60	3.52	4.0	4.31	...	4.59	5.08
$2p_9$	5.06	5.15	4.44	3.28	5.13	4.2	5.4	5.24
$2p_{10}$	3.78	4.04	3.65	2.33	...	3.8	3.28 ^a	...	3.27 ^a	3.96

^aContribution of weak line of order 1% is missing.

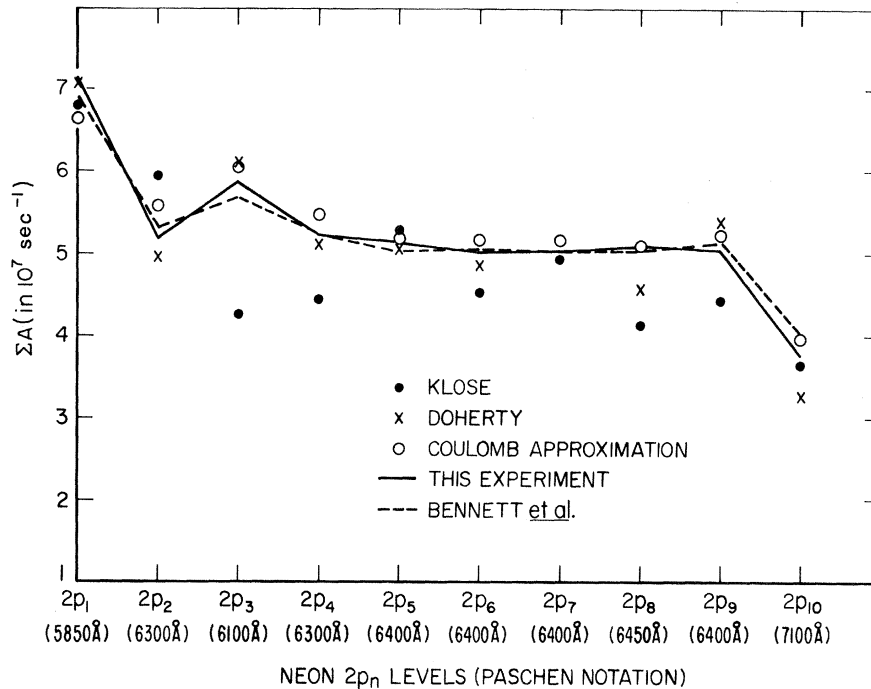


FIG. 1. Transition probabilities versus index of upper energy levels.

ities. All the remaining data exhibit scatter which is still larger than that for the presented work (as may be seen from Table V).

All the data sets show an irregular trend towards smaller transition-probability sums with increasing index of the p levels. This is readily understood on the following grounds: Since σ^2 , and therefore the line strengths, are approximately constant within the array (Table IV), the transition probability is essentially inversely proportional to λ^3 [see Eq. (2)]. The approximate mean wavelengths for the transitions from the various p levels are shown on the bottom of Fig. 1, and it is seen that they increase in the same irregular fashion with the numbers of the p levels as ΣA decreases.

Table V shows also that a somewhat more pronounced trend is noticeable in the data of Denis *et al.*, Bengtson and Miller, and Nodwell *et al.*, which implies a systematic variation in σ^2 . This has already been encountered in connection with the data listed in Table III. Such a trend, for the emission experiments, could be caused by systematic errors in the temperature determination and the spectral intensity calibration, since the excitation energies as well as the wavelengths vary sufficiently within the transition array to possibly cause a trend of this magnitude. Also, self-absorption effects could be responsible, because the lines associated with the higher-index p levels are of increasingly stronger intensity, i.e., they possess the largest $g_k A_{ki}$ values. This latter effect

of "radiative imprisonment" could, of course, also be present in the lifetime experiments. We have generally found in the papers of the above-mentioned authors that they have made checks on self-absorption. However, small effects of the magnitude required to explain the trends could go undetected. Bakos and Szigeti¹² have apparently observed the radiative imprisonment effects quite clearly, since they find shorter lifetimes with decreasing pressure.

CONCLUSIONS

We have measured the relative transition probabilities of all lines of the Ne I $3s-3p$ array and have combined our individual values with the absolute transition-probability sums determined from the accurate lifetime experiment of Bennett and Kindlmann¹⁷ to present a new set of accurate transition probabilities (Table I, this expt. I). We have subjected our results, as well as earlier emission experiments, to several spectroscopic tests which indicate a much higher degree of consistency in our data than in any of the others. Based principally on these checks, as well as our experimental-error analysis and the error estimates by Bennett and Kindlmann, we expect the new set of transition probabilities to be accurate to within 10%, except for the very weak lines, where it should be 15%.

We gratefully acknowledge the assistance of R. L. Kornblith in the preliminary phases of the experiment.

*Research supported in part by the Advanced Research Projects Agency of the Department of Defense under the Strategic Technology Office.

¹W. L. Wiese, M. W. Smith, and B. M. Glennon, *Atomic Transition Probabilities* (U. S. GPO, Washington, D. C., 1966), Vol. I, NSRDS-NBS 4.

²K. Krebs, *Z. Physik* 101, 604 (1936).

³R. Ladenburg and S. Levy, *Z. Physik* 88, 461 (1934).

⁴A. Pery-Thorne and J. E. Chamberlain, *Proc. Phys. Soc. (London)* A82, 133 (1963).

⁵L. R. Doherty, thesis, Michigan University, 1961 (unpublished).

⁶M. Garbuny, *Z. Physik* 107, 362 (1937).

⁷H. Friedrichs, *Z. Astrophys.* 60, 176 (1964).

⁸J. Z. Klose, *Phys. Rev.* 141, 181 (1966); in *Beam Foil Spectroscopy* (Gordon and Breach, New York, 1968), p. 285.

⁹W. R. Bennett, Jr., P. J. Kindlmann, and G. N. Mercer, *Appl. Opt. Suppl.* 2, 34 (1965).

¹⁰D. R. Bates and A. Damgaard, *Phil. Trans. Roy. Soc. London* A242, 101 (1949).

¹¹A. Denis, J. Desesquelles, and M. Dufay, *Compt. Rend.* 266B, 1016 (1968).

¹²J. Bakos and J. Szigeti, *Acta Phys. Acad. Sci. Hung.* 23, 341 (1967).

¹³T. Krupenikova and M. Chaika, *Opt. i Spektroskopiya* 20, 1088 (1966) [*Opt. Spectry. (USSR)* 20, 604 (1966)].

¹⁴A. L. Osherovich and Ya. F. Verolainen, *Opt. i Spektroskopiya* 22, 329 (1967) [*Opt. Spectry. (USSR)* 22, 181 (1967)].

¹⁵D. Rosenberger and I. Thumb, *Z. Naturforsch.* 21a, 175 (1966).

¹⁶T. H. Hänsch and P. Toschek, *Phys. Letters* 20,

273 (1966).

¹⁷W. R. Bennett, Jr. and P. J. Kindlmann, *Phys. Rev.* 149, 38 (1966).

¹⁸R. A. Nodwell, H. W. H. Van Andel, and A. M. Robinson, *J. Quant. Spectry. Radiative Transfer* 8, 858 (1968).

¹⁹J. C. Irwin and R. A. Nodwell, *Can. J. Phys.* 44, 1781 (1965).

²⁰R. D. Bengtson and M. H. Miller, *J. Opt. Soc. Am.* 60, 1093 (1970).

²¹W. Seka and T. L. Curzon, *J. Quant. Spectry. Radiative Transfer* 8, 1147 (1968).

²²See, e.g., W. L. Wiese, in *Methods of Experimental Physics*, Vol. 7A (Academic, New York, 1968), Chap. 2.1.

²³D. R. Paquette and W. L. Wiese, *Appl. Opt.* 3, 294 (1964).

²⁴See, e.g., W. L. Wiese, in *Methods of Experimental Physics*, Vol. 7B (Academic, New York, 1968), Part 10.

²⁵J. Richter, *Z. Astrophys.* 61, 57 (1965).

²⁶G. D. Bell, D. R. Paquette, and W. L. Wiese, *Astrophys. J.* 143, 559 (1966).

²⁷C. W. Allen, *Astrophysical Quantities*, 2nd ed. (The Athlone Press, London, 1963).

²⁸B. W. Shore and D. H. Menzel, *Principles of Atomic Spectra* (Wiley, New York, 1968), p. 447.

²⁹R. Mehlhorn, *J. Opt. Soc. Am.* 59, 1453 (1969).

³⁰R. I. Semenov and B. A. Strugach, *Opt. i Spektroskopiya* 24, 487 (1968) [*Opt. Spectry. (USSR)* 24, 258 (1968)].

³¹G. H. Shortley, *Phys. Rev.* 47, 295 (1935).